# One-dimensional spin-anisotropic kinetic Ising model subject to quenched disorder

Nóra Menyhárd[1] and Géza Ódor[2]
[1]*Research Institute for Solid State Physics and Optics, H-1525 Budapest, P.O. Box 49, Hungary*
[2]*Research Institute for Technical Physics and Materials Science, H-1525 Budapest, P.O. Box 49, Hungary*
(Received 21 December 2006; revised manuscript received 4 June 2007; published 2 August 2007)

Large-scale Monte Carlo simulations are used to explore the effect of quenched disorder on one-dimensional, nonequilibrium kinetic Ising models with locally broken spin symmetry, at zero temperature (the symmetry is broken through spin-flip rates that differ for "+" and "−"spins). The model is found to exhibit a continuous phase transition to an absorbing state. The associated critical behavior is studied at zero branching rate of kinks, through analysis spreading of + and − spins, and of the kink density. Impurities exert a strong effect on the critical behavior only for a particular choice of parameters, corresponding to the strongly spin-anisotropic kinetic Ising model introduced by Majumdar *et al.* [Phys Rev. Lett **86**, 2301 (2001)]. Typically, disorder effects become evident for impurity strengths such that diffusion is nearly blocked. In this regime, the critical behavior is similar to that arising, for example, in the one-dimensional diluted contact process, with Griffiths-like behavior for the kink density. We find variable cluster exponents, which obey a hyperscaling relation, and are similar to those reported by Cafiero *et al.* [Phys Rev. E **57**, 5060 (1998)]. We also show that the isotropic two-component $AB\rightarrow\emptyset$ model is insensitive to reaction disorder, and that only logarithmic corrections arise, induced by strong disorder in the diffusion rate.

DOI: 10.1103/PhysRevE.76.021103 PACS number(s): 05.70.Ln, 05.70.Fh, 05.70.Jk, 82.20.Wt

## I. INTRODUCTION

The study of nonequilibrium model systems has attracted great attention in recent years. A variety of phase transitions have been found characterized by critical exponents, both static and dynamic. Of special interest are transitions from a fluctuating active state into an absorbing one. A wide range of models with transitions into absorbing states was found to belong to the directed percolation (DP) universality class [1,2]. Another universality class of interest is the so-called parity conserving (PC) class [3–6]. The most extensively studied model in this class is branching annihilating random walks with an even number of offsprings (BARWe) in one dimension. The first examples of models exhibiting a PC-type transition were two one-dimensional cellular automata studied by Grassberger [7]. The prototype *spin* model for PC-type phase transitions, the nonequilibrium kinetic Ising model (NEKIM), was proposed by one of the authors [8]. In this model domain walls (kinks) between unlike spins follow BARWe dynamics.

One-dimensional models showing DP transition, such as the contact process, exhibit pronounced changes in behavior under the effect of quenched spatial disorder, even for small impurity concentrations (see [9] and references there). On the other hand, as a recent computer simulation study [10] has shown with great accuracy, the parity-conserving class appears to be highly resistant to impurities. The same study reported similar, or even stricter, negative results for the one-dimensional Glauber-Ising model [11].

Another aspect of the problem, however, was identified by Majumdar *et al.* [12], who introduced a specific, inherent spin anisotropy (kinetic disorder) in the Glauber-Ising model [Majumdar Dean Grassberger (MDG) model in the following]. These authors found, both analytically and numerically, a slow logarithmic factor in the decay of the density of kinks $\rho(t)$ for $t\rightarrow\infty$.

The aim of the present study is to show that in certain Ising-like systems (possessing two absorbing states), local kinetic disorder may effectively remove one of the absorbing states. The resulting, single-absorbing state system is sensitive to spatial disorder, similar to models in the directed percolation class. To this end we start from a generalization of NEKIM, the nonequilibrium kinetic Ising model with anisotropy (NEKIMA) [13,14], with variable kinetic disorder, and add uncorrelated spatial impurities to the system. We recall that without spatial impurities and in the zero-branching limit considered throughout this paper, the exponent $\alpha$, which governs the time dependence of the kink density, $\rho(t)\sim t^{-\alpha}$, is invariably $\alpha=1/2$ (apart from possible logarithmic corrections). The characteristic cluster exponents, which are more susceptible to kinetic disorder than those governing the kink density, differ, however, from their Glauber-Ising values. This phase will be called spin-anisotropic Glauber-Ising (SAGI). For definitions and details of the models referred to here, and the acronyms used, see Table I.

Our numerical studies show that the scaling behavior of the SAGI phase is resistant to quenched spatial impurities, of strength $p_0$, in the small-impurity regime. Close to the incipient freezing of a diffusion channel, which occurs at about $p_0=0.5$, and which appears to be a dirty critical point [9], the exponent $\alpha$ jumps from 0.5 to 0.21. On increasing $p_0$ further, a Griffiths-like [15] phase is encountered, with $\alpha(p_0)$ increasing with $p_0$. The cluster properties: the mean population size $n(t)\sim t^{\eta}$, the mean-square distance of spreading of spins $R^2(t)\sim t^z$, and the survival probability, $P(t)\sim t^{-\delta}$ are also found to change from their SAGI expressions (Table II) to those characteristic of a Griffiths phase [15]. We find close similarities to the results on scaling in the impure contact process [16] in (almost) the whole plane of the corresponding phase diagram, with the hyperscaling law remaining valid. Here this behavior is found in an annihilating random-walk-type model (ARW) i.e., without kink production, while

 

TABLE I. Summary of models. Here $w$ denotes the spin transition probabilities, $A=\Gamma(1+\tilde{\delta})$, $B=\Gamma/2(1-\tilde{\delta})$.

| Transition probability | $w(+,--)$ | $w(-,++)$ | $w(-,+-)=w(-,-+)=p$ | $w(+,+-)$ $w(+,-+)=p_+$ | $w_{ex}(s_i,s_{i+1})=p_{ex}(1-s_is_{i+1})$ | Kink dynamics |
|---|---|---|---|---|---|---|
| Glauber-Ising | $A$ $\tilde{\delta}\geqslant 0$ | $A$ $\tilde{\delta}\geqslant 0$ | $B$ | $B$ | 0 | ARW |
| NEKIM | $A$ $\tilde{\delta}<0$ | $A$ $\tilde{\delta}<0$ | $B$ | $B$ | $\neq 0$ | PC |
| NEKIMA | $A$ $\tilde{\delta}=0$, $\Gamma=1$ | 0 (MDG) | $p$ (=1/2) | $p_+=p=1/2$ (MDG) $p_+<p$ (SAGI) | $\neq 0$ 0 | DP SAGI |
| NEKIMCA CA update | $A$ | $A$ | $B$ | $B$ | 0 | PC |

production takes place on the level of spins, in one of the spin channels ("+" spins in the following), as explained in Sec. II.

Moreover, in the present case the SAGI phase plays the role of a supercritical phase: activelike concerning + cluster behavior while frozen for the "−" spin phase, and of annihilating-random-walk type for the kink density $\rho(t)$. The dual nature of global and cluster properties is not contradictory and can be traced back to the fact that the model is highly spin anisotropic.

The NEKIMA model coincides, at some specific parameter values (MDG case, Fig. 1) with the model of Majumdar *et al.* [12] mentioned above. The joint effect of kinetic and spatial impurities is even more pronounced at and in the vicinity of this point (see the phase diagram depicted in Fig. 1, where the most spin-anisotropic point, the MDG point, is at the origin). In this region of the $(p_+,p_0)$ plane the impure scaling behavior is different: by increasing $p_0$ we have found a change in the behavior of the global quantity $\rho(t)$: $\alpha$ switches from a value of 1/2 (apart from the very late time logarithmic correction) to $\alpha=1$. The cluster behavior is different for the + and − spins. For the + it appears to follow the above mentioned scheme [16] of the impure contact process: upon increasing $p_0$ a strong tendency towards the absorbing + phase can be seen with the hyperscaling law [17] satisfied. For the − cluster we find $\eta=z/2=1$, and $\delta=0$, with logarithmic corrections in time.

In summary, we find that by increasing spin anisotropy the sensitivity of critical behavior to quenched disorder is enhanced (NEKIM→SAGI→MDG). It is worth noting that in order to maintain the symmetry of the NEKIMA model, the disorder affecting diffusion is anisotropic too, therefore it is different from the problem considered in [10], where for very strong disorder diffusion can be blocked completely.

In the Appendix a further, isotropic ARW model, $AB\rightarrow\emptyset$ [1], is investigated via numerical simulations, under quenched disorder. In this model, which can be mapped onto the pure MDG model [2] the effect of impurities on the annihilation and diffusion rates are investigated separately: the density decay is unaffected in case of the former, while logarithmic corrections arise for impure diffusion rates for very long times.

The paper is organized as follows. In Sec. II we define the models and the quantities to be investigated. Some previous results for the exponents of spreading from a localized source are recalled and commented on. In a subsection—to enlighten the different roles played by the + and − spins—our model is mapped onto a reaction-diffusion system. In Sec. III the effect of spatial impurities is investigated for two different choices of the value of the anisotropy parameter: the SAGI case (A) and the more spin-anisotropic MDG case (B). The results are discussed in Sec. IV, while in the Appendix a further ARW model, the $AB\rightarrow\emptyset$, is investigated under the influence of quenched disorder.

## II. SPIN-ANISOTROPIC GLAUBER-ISING MODEL

In the one-dimensional Glauber model at zero temperature, the most general form for the flipping rate of spin $s_i$ is [11] ($s_i=\pm 1$)

$$w(s_i,s_{i-1},s_{i+1})=\frac{\Gamma}{2}(1+\tilde{\delta}s_{i-1}s_{i+1})\left(1-\frac{1}{2}s_i(s_{i-1}+s_{i+1})\right). \quad (1)$$

Usually the Glauber model is understood as the special case $\tilde{\delta}=0$, $\Gamma=1$ and we will use these parameter values in the following. Processes involving the reaction one kink→three kinks are introduced via the exchange rate

TABLE II. Cluster critical exponents at the SAGI transition point and at the MDG point.

| Exponents | SAGI + | SAGI − | MDG + | MDG − | Diso MDG + | Diso MDG − |
|---|---|---|---|---|---|---|
| $\eta$ | 1 | 0 | 0 | 0.5 | −1 | 1 |
| $\delta$ | 0 | 0 | 0.5 | 0 | 1 | 0 |
| $z$ | 2 | 0 | 1 | 1 | 0 | 2 |

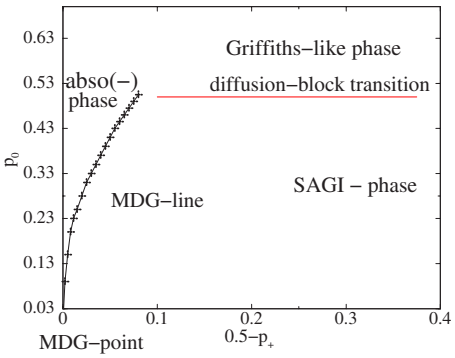


FIG. 1. (Color online) Phase diagram of the impure NEKIMA model ($p_{ex}=0$, ARW case). Different regions of behavior are marked (for details see text). The vicinity of $p_+=0$ is not shown as it is not discussed here.

$$w_{ex}(s_i,s_{i+1}) = \frac{p_{ex}}{2}(1 - s_i s_{i+1}) \tag{2}$$

(a kink is a $-+$ or $+-$ configuration: the domain boundary between two oppositely magnetized regions). For negative values of $\tilde{\delta}$ this model (called NEKIM) shows a line of PC transitions in the $(p_{ex}, \tilde{\delta})$ plane [8]. The NEKIMA model is an extension with local symmetry breaking in the flipping rates of the $+$ and $-$ spins as follows. Concerning the annihilation rates (of a spin in the neighborhood of oppositely oriented spins) the prescription in [12] is followed:

$$w(+;--) = 1, \quad w(-;++) = 0. \tag{3}$$

Further spin symmetry breaking is introduced in the diffusion part of the Glauber transition rate as follows. The transition rates

$$p \equiv w(-;+-) = w(-;-+) = \Gamma/2(1 - \tilde{\delta}) \tag{4}$$

are taken as in Eq. (1), while $w(+;+-)$ and $w(+;-+)$ may take smaller values:

$$p_+ \equiv w(+;+-) = w(+;-+) \leqslant p. \tag{5}$$

In this way, by locally favoring $+$ spins, the effect of the other dynamically induced field arising from the rates [Eq. (3)] is counterbalanced. The spin-exchange part of the NEKIM model remains unchanged [Eq. (2)].

Spreading from a localized source at criticality is usually described by the following three quantities:

$$P(t) \sim t^{-\delta},$$

$$n(t) \sim t^{\eta},$$

$$R^2(t) \sim t^{z}, \tag{6}$$

where $n(t)$ denotes the mean population size, $R^2(t)$ is the mean square spreading of particles (here spins) about the origin, and $P(t)$ is the survival probability. In most cases these quantities are defined for particles, in the present case, however, they will be used for spins.

In NEKIMA $+$ and $-$ spins are not symmetric, therefore we have investigated two kinds of clusters. Namely, the development of the $-$ cluster seed was started from a wholly $+$ environment while that of the $+$ cluster was started from a sea of $-$ spins. We will call them the $-$ cluster and the $+$ cluster, respectively. The cluster critical exponents for the NEKIMA were reported in [14]. Their values at a typical SAGI point ($p_+=0.3$, $p=0.5$) and at the MDG point ($p_+=p=0.5$), for the ARW case discussed here, are summarized on Table II. It should be noted here, however, that the precision of the simulations in the above cited paper does not exclude the possibility of the presence of some $\log(t)$ corrections.

On the level of $+$ spins the SAGI phase ($1/2=p>p_+$) is an active one as shown by the $+$ cluster exponents in Table II. For producing $+$ spins the rate in Eq. (4) with $p=1/2$ is responsible, while $p_+$ annihilates them. Crudely speaking, the probability of the $+$ spin-generating transition process, $p-p_+$, can be thought of as the quantity corresponding to the particle production rate in the contact process.

As one can see, due to the anisotropies the $-$ and $+$ spins follow different dynamics. To understand the peculiar behavior of the species we transform their motion into the language of reaction-diffusion models, making a connection with the basic models and classes [2].

### Particle picture of the spin processes

Let $X$ be a particle and $\emptyset$ its absence. For the $-$ spins as X's and $+$ spins as $\emptyset$'s, Eq. (3) gives

$$X\emptyset X \to XXX \tag{7}$$

creation, while Eq. (5) leads to the creation

$$X\emptyset\emptyset \to XX\emptyset, \quad \emptyset\emptyset X \to \emptyset XX. \tag{8}$$

From the above three, the net process remains as

$$\emptyset X \to XX. \tag{9}$$

Similarly Eq. (4) means the coagulation processes,

$$\emptyset XX \to \emptyset\emptyset X, \quad XX\emptyset \to X\emptyset\emptyset. \tag{10}$$

From Eqs. (9) and (10) the generic reactions

$$X \leftrightarrow 2X \tag{11}$$

follow. This corresponds to the recently studied reversible model [18–21], where transition to an absorbing phase can occur only for zero branching rate, which is excluded in our case, hence we don't expect an active-absorbing phase transition of the '$-$' spins.

On the other hand for the '$+$' spins as X's we get from Eq. (3) the

$$\emptyset X\emptyset \to \emptyset\emptyset\emptyset \tag{12}$$

spontaneous decay and from Eq. (5) the coagulation

$$\emptyset XX \to \emptyset\emptyset X, \quad XX\emptyset \to X\emptyset\emptyset, \tag{13}$$

while Eq. (4) gives the creation by a neighbor

$$X\emptyset\emptyset \to XX\emptyset, \quad \emptyset\emptyset X \to \emptyset XX \tag{14}$$

These give again $XX \leftrightarrow X$ but according to Eq. (12) here the spontaneous annihilation of X, $X \to \emptyset$ is also possible due to Eq. (3), which is a necessary condition for a DP class transition. Hence for '+' spins a phase transition (at finite reaction rates) is not excluded and as we will see later it emerges as the effect of the disorder. The corresponding critical behavior is similar to that of the disordered DP (albeit an anisotropic one).

## III. EFFECTS OF QUENCHED IMPURITIES

At each site $i$ the diffusion rates of kinks $p=w(-;+-)=w(-;-+)$ in Eq. (4) are modified by adding quenched, uncorrelated impurities with uniform probability distribution of the form

$$p_i = p + p_0[2\epsilon(i) - 1], \tag{15}$$

where $\epsilon(i)$ is randomly distributed in the interval $0 \leqslant \epsilon(i) \leqslant 1$ and $0 \leqslant p_0 \leqslant 0.5$. On the other hand, the rates, which fix the (a)symmetry of the model $w(+;--)=1$, $w(-;++)=0$, and $p_+$ of Eq. (15), are kept uninfluenced. In this way kinetic impurities and quenched local impurities are allowed to act separately, though simultaneously, resulting in a rich phase diagram.

Two characteristic impure behaviors are exemplified by the following two choices of the fixed parameters: (i) $p_+=0.3$ (to be called the SAGI case) and (ii) $p_+=0.5$ (to be called the MDG case).

The phase diagram of the impure NEKIMA is shown schematically in Fig. 1. At the MDG point the $-$ phase gets dominating (Sec. III B.). This absorbing $-$ phase is separated from the SAGI phase by the MDG line, a line of critical points characterized by the cluster exponents given in Table II and where $\alpha=1/2$. This line is depicted here only tentatively (especially for higher $p_0$ values), as its neighborhood is not the subject of our further detailed study. The diffusion-block transition line corresponds to the limiting value: $p_0=1/2$, where the only nonfixed spin-flip probability can become zero, hence diffusion blocking starts. The SAGI phase in the vicinity of this point will be discussed in the next section. It is worth emphasizing again that in the present model only one transition probability gets impure (one spin-flip rate) in contrast to a previous investigation of NEKIMCA with impurities [10], where all four transition rates (spin-flip+annihilation) have been complemented with a term like that in Eq. (15). We have also looked into the effect of impurities in one of the annihilation rates of the two fixing the model's anisotropy: no effect shows up in the vicinity of $p_0=0.5$ in this case as can be expected.

### A. The SAGI case ($p_+=0.3$)

We will investigate the effect of impurities below the MDG point, i.e., for $p_+<0.5$ at a typical parameter value $p_+=0.3$ (see Fig. 1) by simulating a system of size $L=3\times10^4$ with periodic boundary conditions up to $t_{max}=10^6$ Monte Carlo steps (MCS's) (throughout the paper, time is measured by MCS's). For small impurity rates $p_0$ the behavior is found unperturbed. Correspondingly, the critical exponent of the density of kinks as a function of time is $\alpha=1/2$ and the exponents of the $+$ and $-$ clusters are as seen in Table II. By increasing $p_0$, the rate of disorder, however, the spin flip rate $p_i$ in Eq. (15) can become zero in the vicinity of $p_0=0.5$ and above. To interpret the results in this region it is important to recall [14] that the critical behavior of the kink density and that of the $+$ and $-$ clusters are not connected in the present model (thus no scaling law connects the critical dynamical exponent $Z$ and the cluster size exponent $z$). While there is no particle production on the level of kinks (ARW process), on the level of spins there is production as mentioned in the previous section. The spin-transition rate $p$, for the process $(--+)\to(-++)$, leads to the increase of $+$ spins. This $+$-spin production is maximal at $p_0=0$. The SAGI phase is an active one, more precisely a $+$-active one (the $-$-spin phase is frozen). At the same time in the usual sense of Glauber-Ising-type models, on the level of kinks, there is no active phase as the kink production $p_{ex}$ in Eq. (2) is zero.

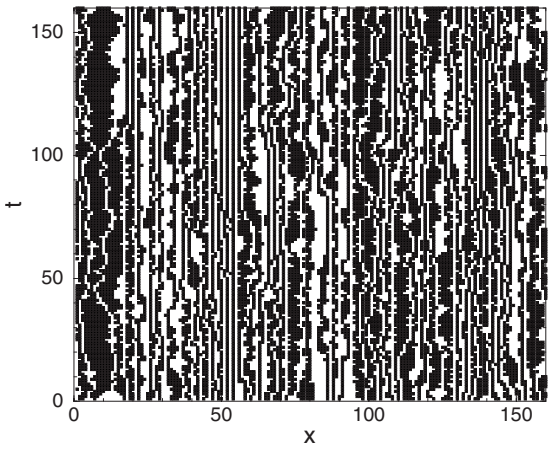


FIG. 2. Space-time picture at $p_+=0.3$, $p_0=0.5$ (disordered SAGI) starting from a random initial distribution of $+$ and $-$ spins. The $+$'s are black

By increasing $p_0$ the system stays in this $+$-active phase, neither the kink-decay exponent $\alpha=1/2$ nor the cluster exponents of Table II change. Approaching $p_0=1/2$, however, the impure spin-flip term $p_i$, Eq. (15), can become zero at certain sites and the process diagram becomes as shown in Fig. 2. The presence of active zones between otherwise frozen-in strips is clearly seen there. The similarity to the time-evolution pictures (Fig. 3 in [22]) showing growth of DP clusters in the impure active and glassy phases is evident. These can be thought of as the much-cited active zones of the impure contact process [9,16,22,23] inside of the otherwise inactive substrate. Thus we can expect similar impure critical behavior to take place. This means the generic presence of scale invariance, and the existence of a sublinear growth regime. This regime is entered now from the active one by increasing $p_0$, through the "dirty" critical point at $p_0=0.5$ (no clean critical point exists in our case, of course). In the vicinity of $p_0=0.5$ the local exponent values defined as

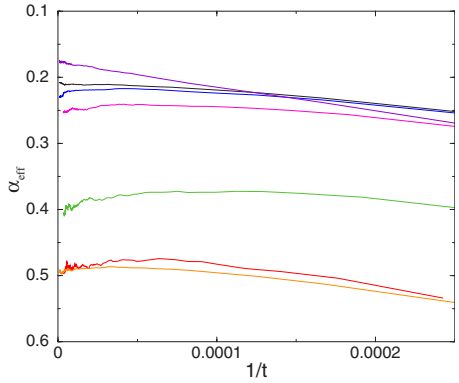


FIG. 3. (Color online) Local exponent values of the kink density in the disordered SAGI phase for different values of the impurity strength $p_0$=0.56, 0.501, 0.503, 0.499, 0.47, 0.4, and 0.1 (top to bottom).

$$\alpha_{eff}(t) = \frac{-\ln[\rho(t)/\rho(t/m)]}{\ln(m)} \tag{16}$$

(where we used $m$=4) behave as in Fig. 3. The fixed point value of the density of kinks at $p_0$=0.5 can be fitted with a power of $\ln(t)$,

$$\rho(t) \sim (\ln t)^{-\tilde{\alpha}}, \tag{17}$$

with $\tilde{\alpha}$=1.459 43 as shown in Fig. 4. This exponent differs from that of the known value of the infinite randomness fixed point of the (1+1) dimensional [(1+1)D] DP ($\tilde{\alpha}_{DP}$ =0.381 97) [24], not surprisingly, kinks follow an anisotropic dynamics here. The excellent fit with Eq. (17) suggests that this point is a dirty critical point, which is reached from the "active" phase (here from the +-active phase). The value of $\alpha$ is a new critical exponent. For higher values of impurity strength a Griffiths-like phase with

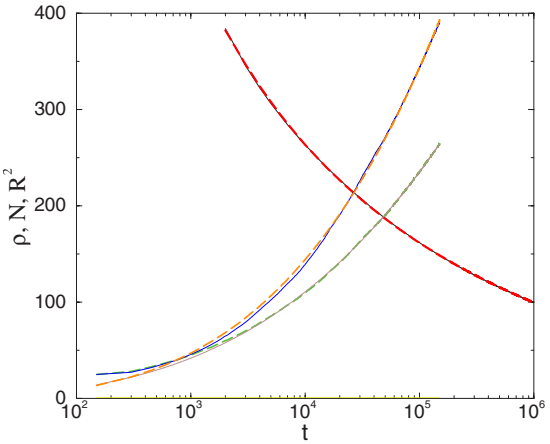


FIG. 4. (Color online) The "dirty critical point" of the intermediate SAGI phase entered by increasing $p_0$ at $p_0$=0.5 is demonstrated by this fit. The decreasing curve corresponds to the kink density; the higher increasing curve shows the spreading radius $R^2$, while the lower increasing one shows the spin number $N$ of +-spin domains. The dashed lines on top of the solid ones show activated scaling fit of the form (17).

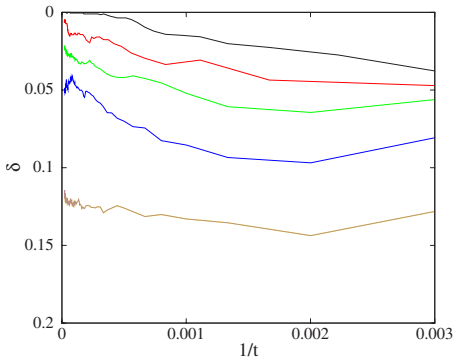


FIG. 5. (Color online) Local exponent values of $P(t)$ of the + clusters in the disordered SAGI phase for $p_0$ =0.47, 0.5, 0.51, 0.525, 0.56 (from top to bottom).

$$\rho(t) \sim t^{-\alpha(p_0)} \tag{18}$$

is entered. Though in this region the present formulation of the impure problem already goes beyond its range of validity, however, the tendency of the impure behavior is well exhibited in our simulations [e.g., $\alpha(p_0)$ increases steadily as expected in a Griffiths phase, etc.]. Nevertheless, we refrain from giving more details.

The time dependences of the + and − cluster quantities [Eqs. (6)] also show a behavior characteristic of an impure phase transition. The behavior of the − cluster shows an effect of "melting:" $\eta$ and $z/2$ move from 0 to some finite values, upon increasing $p_0$, while $\delta$=0 remains the same. The + cluster behavior, however, shows a scenario of a transition to an absorbing state, similarly to the contact process investigated by Cafiero *et al.* [16]. However, the direction is opposite: in [16] for small values of disorder (called $p$ in their paper) an absorbing phase is present, while the active is reached at $p$=1.

We plot in Fig. 5 the + cluster behavior, namely the local exponent values of the survival probability defined as

$$\delta_{eff}(t) = \frac{-\ln[P(t)/P(t/m)]}{\ln(m)} \tag{19}$$

for different values of disorder. One can clearly see a turn from the SAGI-active behavior ($\delta$=0) towards a Griffiths-phase-like nonuniversal cluster scaling by increasing $\delta$ in the vicinity of $p_0$=0.5.

At $p_0$=0.5 (dirty critical point of the + spins) an ultraslow, activated scaling of the form Eq. (17) can be observed in the cluster data (see Fig. 4). Fitting with the activated scaling forms

$$\delta(t) \sim (\ln t)^{-\tilde{\delta}}, \quad R^2(t) \sim (\ln t)^{\tilde{z}}, \quad N(t) \sim (\ln t)^{\tilde{\eta}}, \tag{20}$$

for the + data resulted in $\tilde{\delta}$=0.060(6), $\tilde{z}$=3.88(1), and $\tilde{\eta}$ =3.37(2). These values again differ from those of the strong disorder fixed point of DP, probably due to the anisotropies of the processes.

Our simulation data for the mean size of the + cluster $R(t)$ depicted on a double-logarithmic scale are shown in Fig. 6. The linear SAGI behavior crosses over to decreasing val-

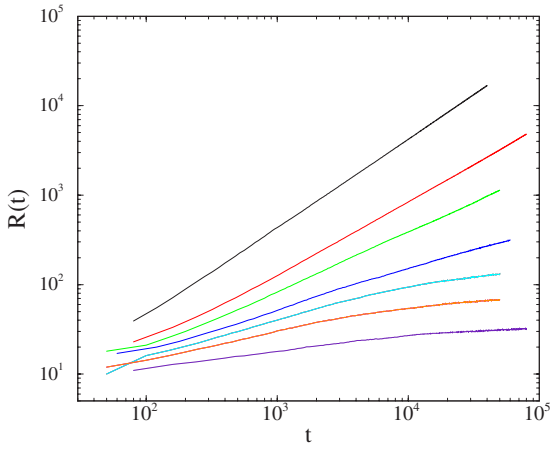


FIG. 6. (Color online) $\ln R(t)$ vs $\ln(t)$ for the + cluster in the SAGI phase for $p_0=0.3,0.45,0.48,0.5,0.52,0.55,0.56$ (top to bottom).

ues of $z/2$ by reaching the $p_0=0.5$ transition point (sublinear behavior; for similar behavior, see Tables I and II in [16]).

### B. The MDG case ($p_+=0.5$)

The MDG point can be found at the origin of the phase diagram (Fig. 1). At these parameter values the impure system decays into a fully compact state, where all spins are flipped to − but different types of kinks exert marginal perturbation on each other [25]. In more detail [12], found analytically that the magnetization decays as

$$m(t) = -1 + \text{const}/\ln(bt), \tag{21}$$

while the kink density behaves as

$$\rho(t) \sim t^{-1/2} \ln(bt) \tag{22}$$

(where $b$ is constant). For the time being—since much stronger (power-law-type) effects enter due to the quenched spatial impurities—we disregard the $\ln(t)$-type of correction and show only the leading singular behavior of the cluster properties (see Table II).

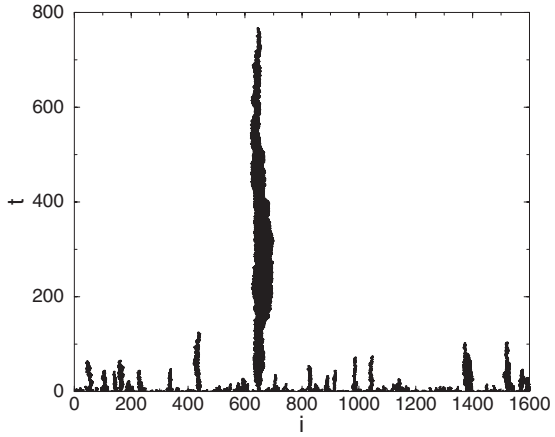


FIG. 7. Space-time evolution in the disordered MDG model ($p_+=0.5$, $p_0=0.3$) from the random initial configuration. The + (black) and − (white) spin clusters are separated by kinks.

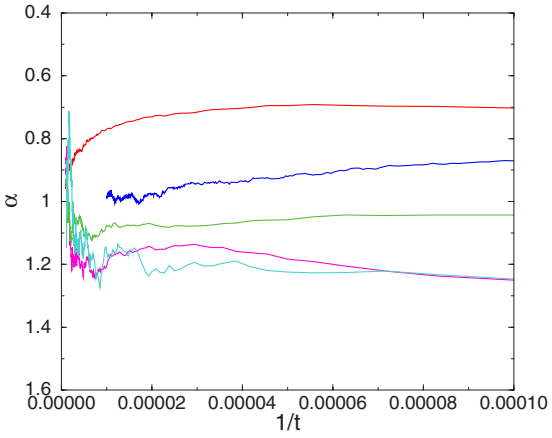


FIG. 8. (Color online) Local exponent values of $\rho(t)$ for different values of $p_0=0.08,0.18,0.25,0.45,0.5$ (from top to bottom) indicating $\alpha=1$-type power-law behavior.

By introducing impurities of strength $p_0=0.3$, the space-time evolution of kinks looks as can be seen in Fig. 7. The absorbing nature of the + phase is apparent. The fully − spin configuration sets in quickly (compare this figure with Fig. 1 of [14], where single − spins move via random walk in the sea of +'s).

Results of high-precision simulations are shown in Fig. 8. For $p_0<0.5$ one can see $\alpha\to 1$ in the long time limit. This behavior can be ascribed to the choice of the impurity, which acts against one type of diffusion (which favors + spins). As a consequence the −'s can spread better than in the impure case. The effect of impurities on the − clusters is illustrated in Fig. 9 for the $\eta$ and $z/2$ exponents. The local slope curves of $\eta$ and $z/2$ are almost the same, they approach the asymptotic value $\eta=z/2=1$ from below with an upward curvature ($\delta=0$ remains constant). This kind of effective exponent behavior usually corresponds to logarithmic correction to scaling. In the case of the general form for $N(t)$,

$$N(t) = t^{\eta} \ln^{b}(t), \tag{23}$$

the effective exponent behaves as

$$\eta_{eff} = \frac{d \ln[N(t)]}{d \ln(t)} = \eta + \frac{b}{\ln(t)}. \tag{24}$$

Therefore a logarithmic fit of the form

$$a + b/\ln(t) \tag{25}$$

has been applied for the local exponent curves and the values obtained both for $\eta$ and $z/2$ are shown in Table III. The clusters are compact, of course, thus the hyperscaling law is satisfied.

TABLE III. Logarithmic fitting results for the − spins clusters at the MDG point for various disorders via Eq. (25).

| | $p_0=1$ | $p_0=0.56$ | $p_0=0.35$ |
|---|---|---|---|
| $\eta=z/2$ | 1.001(1) | 1.004(5) | 0.95(6) |
| $b$ | −1.511 | −1.825 | −1.87 |

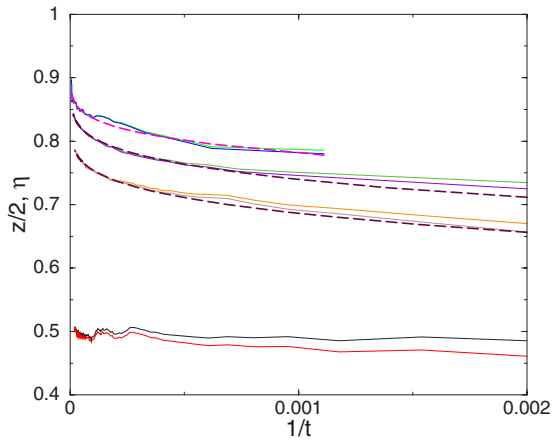


FIG. 9. (Color online) Negative cluster exponents $\eta$ and $z/2$ in the impure MDG case for $p_0=1,0.56,0.35,0$ (in pairs, from top to bottom). $\delta=0$ $[P(\infty)=1]$ in the whole interval. The dashed lines are logarithmic fitting of the form (25).

To summarize, instead of the weak logarithmic tendency towards the dominance of the $-$'s as for the pure MDG model, the impurity pushes the system into a more anisotropic decay, characterized by the kink decay exponent $\alpha=1$. The depletion of the $+$ cluster is illustrated in Figs. 10 and 11. The $+$ cluster dies out apparently in a power-law manner with the exponents $\eta=-1$, $\delta=1$, and $z/2=0$. These scaling behaviors suggest a transition from one absorbing phase (MDG) to another one as the effect of quenched impurities, which increases anisotropy.

It is worth noting that by switching on the spin-exchange term ($p_{ex}$) in the pure case a quicker dominance of the $-$'s takes place for the same parameter values of the model as here. In that case, no power-law regime is visible (except for some early time transient region and for very low values of the kink production $p_{ex}$) and the absorbing phase sets in exponentially fast typically (see [13]) due to the faster destruction of metastable $+$ domains.

## IV. DISCUSSION AND CONCLUSIONS

In this paper, the problem of the effect of quenched impurities on one-dimensional nonequilibrium Glauber-Ising-type models has been investigated numerically. Our previous study of the same problem, without spin anisotropy, led to the conclusion of a minimal effect [10]. Here the emphasis has been on introducing spin anisotropy, and to give insight into the the joint effect of kinetic and quenched spatial anisotropies. We have restricted our studies to the zero branching rate limit of the model (ARW case). Depending on the ratio of anisotropies in the diffusion and annihilation channels (rates) a variety of behaviors appear when the quenched randomness is turned on, with the inference that some amount of kinetic anisotropy can significantly enhance the influence of quenched spatial anisotropies.

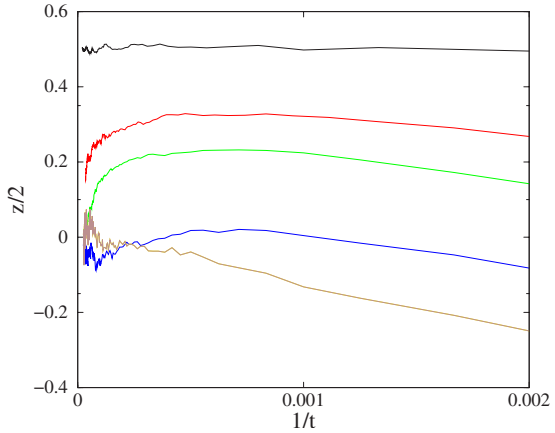


FIG. 10. (Color online) Local exponent values of the $+$ cluster exponent $z/2$ in the impure MDG case for $p_0=0,0.15,0.20,0.35,0.45$ (from top to bottom).

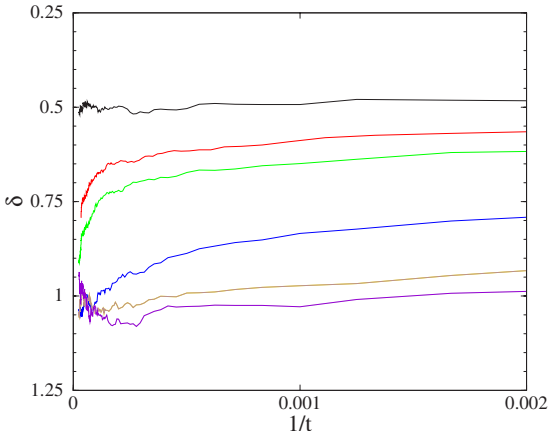


FIG. 11. (Color online) Local exponent values of the $+$ cluster exponent $\delta$ in the impure MDG case for $p_0=0,0.15,0.20,0.35,0.45$ (from top to bottom).

This behavior is different from that found for isotropic NEKIM [10], where reaction and diffusion are completely blocked for very strong disorder. The effects of such blocking are investigated in the context of the $AB\rightarrow\emptyset$ model; only the diffusive ones are found to be marginally relevant.

Summarizing the results for exponents $\eta$, $\delta$, and $z$ (Table II), for $+$ spins in the case $p=p_+=1/2$ (MDG+) we have the $(0,1/2,1)$ spreading fixed point exponents of the $XX\rightarrow X$ diffusive coagulation process, because due to Eq. (3) the $XX\leftrightarrow X$ is unbalanced, favoring $XX\rightarrow X$ annihilation of $+$'s and the proliferation of $-$'s. In the $p_+<p=1/2$ kinetic disorder case (SAGI+) we found [14] a novel kind of anisotropic fixed point (1, 0, 2), which is the same that one obtains if quenched disorder is added to (MDG−). This can be understood by looking closer on the effect of these disorders on the spin species. Both kinds of disorders enhance the production of one species at the expense of the other. While in the case of (SAGI+) the $-$'s are suppressed, for the (diso MDG−) the same thing happens with the $+$'s [due to Eq. (15)] and the other spin domains grow linearly with $\eta=z/2=1$.

However, due to Eq. (3) the handicapped species end up in a different way. In the case of SAGI, the $-$'s can survive, resulting in (0, 0, 0) as $t\rightarrow\infty$, slowing down the domain wall decay (resulting in $\alpha=0.5$). In the case of the diso-MDG the lonely $+$'s can die out completely, characterized by $\eta=-1$ mass and $\delta=1$ survival exponents, enabling the linear growth of kinks. Therefore $\alpha=1$ can be observed here.

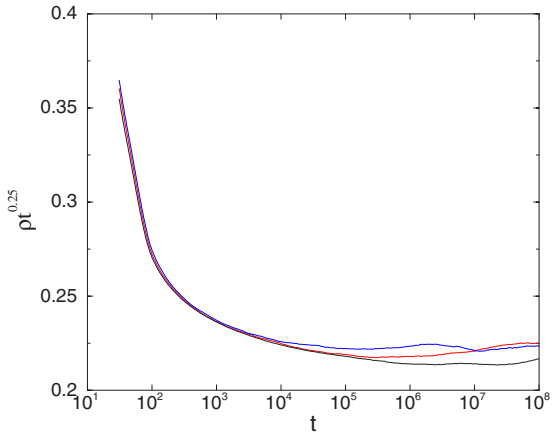


FIG. 12. (Color online) Density decay of the annihilation disordered $AB \to \emptyset$ model in case of RI conditions for $\epsilon_A = 1, 0.98, 0.95$ (top to bottom).

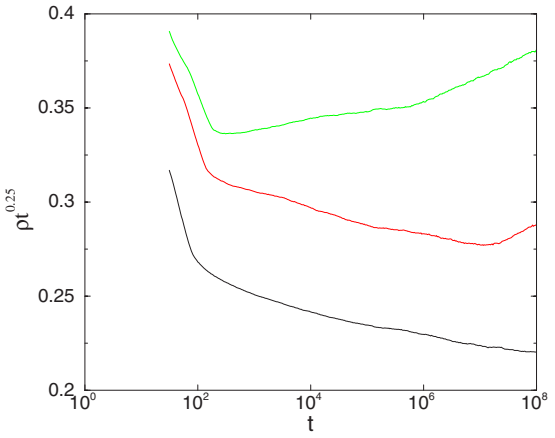


FIG. 13. (Color online) Density decay of the diffusion disordered $AB \to \emptyset$ model in case of RI conditions. Different curves correspond to $\epsilon_D = 1, 0.95, 0.5$ (top to bottom).


## ACKNOWLEDGMENTS

Support from the Hungarian Research Fund OTKA (Grant No. T-046129) during this study is gratefully acknowledged. G.Ó. acknowledges the access to the NIIFI Cluster-GRID, LCG datagrid, and the Supercomputer Center of Hungary.


## APPENDIX

In this Appendix the effect of quenched disorder in a further ARW-type model, the $AB \to \emptyset$ one, will be investigated. Unlike SAGI, this model is free of anisotropies. In our previous paper [10] we investigated the inactive phase of the cellular automaton version of the nonequilibrium kinetic Ising model (NEKIMCA) with quenched disorder. In that model the annihilating random walk of domain walls (kinks) $AA \to \emptyset$ is the dominant process. We have not found any effect of the weak disorder on the density decay of kinks. If the disorder was so strong that diffusion could be blocked at certain sites (the system is split into independent blocks of finite sizes) a new fluctuating phase with finite steady state density emerged as the consequence of the parity conservation of kinks. Along and just below the blocking transition line the disorder caused logarithmic slow-down corrections to the $\rho \propto t^{-1/2}$ impure law of the ARW process [26] and continuously changing exponents ($\alpha < 0.5$) for strong disorder. Those results are in agreement with analytic results for diffusion disorder [27] and annihilation disorder [28] of the ARW.

The anisotropic reactions of the NEKIMA model [13] result in a two component reaction dynamics of kinks destroying the PC class critical behavior. Without kink production ($p_{ex}=0$) one can map onto the $AB \to \emptyset$, however, since $A$ and $B$ species are domain walls of the spins they are arranged alternately along the 1D system. Consequently, they can always meet their nearest neighbors (no hard-core reactions take place as in [29]) and one observes the usual $\rho \propto t^{-1/2}$ decay instead of the $\rho \propto t^{-1/4}$ law of the two component model [30].

In this Appendix we show results for the quenched disordered $AB \to \emptyset$ model to complement results for the quenched disorder NEKIMA model. To our knowledge this has not been studied before. We have investigated the effect of disorder in diffusion and annihilation separately. A random sequential simulation program has been run in 1D systems of size $L = 5 \times 10^5$ with periodic boundary conditions and single particle occupation restriction. We have investigated the density decay for initial conditions with randomly (RI) and pairwisely (PI) distributed $A$'s and $B$'s of full lattice occupancy.

One elementary MC step is built up as follows. A particle and a direction is chosen randomly. If the nearest neighbor (NN) site in the selected direction was empty, the particle is moved there with probability $1-\epsilon_D$ (where $\epsilon_D$ is the diffusion disorder strength). If the NN site was occupied with a particle of a different type we removed both particles with probability $1-\epsilon_A$. The time ($t$) is incremented by $\Delta t = 1/n_p$ (where $n_p$ is the total number of particles) and the density decay was followed up to $t_{max} = 10^8$ MCS's.

In the case of $\epsilon_D = 0$ we did not see any effect of the disorder in the annihilation up to $\epsilon_A \leqslant 1$ both for RI and PI conditions (see Fig. 12 for RI). The density decay is completely insensitive to the quenched randomness of the annihilation reaction rate.

On the other hand, for disorder in the diffusion (hopping) probabilities ($\epsilon_A = 0$, $\epsilon_D \leqslant 1$) one can see logarithmic corrections to the scaling of the impure case for $\epsilon_D \to 1$ (see Fig. 13 for RI). Following a sharp initial decay, when local correlations are built up the evolution tends towards the $\rho \propto t^{-0.25}$ law, but as in the case of the ARW model logarithmic slow-down appears for very late times and strong disorder (already without diffusion blocking). It has been tested by simulating on different sizes ($L$) that the turns in the curves are not artifacts of finite system sizes. Since the basic mechanism of annihilating random walk, here $AB \to \emptyset$, is the same as for the $AA \to \emptyset$ model, we think that the relevancy of diffusion disorder compared to the annihilation disorder can be observed in the inactive phase of the NEKIMCA [10] as well.

[1] For a review, see J. Marro and R. Dickman, *Nonequilibrium Phase Transitions in Lattice Models* (Cambridge University Press, Cambridge, England, 1996); H. Hinrichsen, Adv. Phys. **49**, 815 (2000).
[2] G. Ódor, Rev. Mod. Phys. **76**, 663 (2004).
[3] I. Jensen, Phys. Rev. E **50**, 3623 (1994).
[4] D. Zhong and D. ben-Avraham, Phys. Lett. A **209**, 333 (1995).
[5] M. H. Kim and H. Park, Phys. Rev. Lett. **73**, 2579 (1994).
[6] H. Park, M. H. Kim, and H. Park, Phys. Rev. E **52**, 5664 (1995).
[7] P. Grassberger, F. Krause, and T. von der Twer, J. Phys. A **17**, L105 (1984); P. Grassberger, *ibid.* **22**, L1103 (1989).
[8] N. Menyhárd, J. Phys. A **27**, 6139 (1994).
[9] T. Vojta, J. Phys. A **39**, R143 (2006).
[10] G. Ódor and N. Menyhárd, Phys. Rev. E **73**, 036130 (2006).
[11] R. J. Glauber, J. Math. Phys. **4**, 191 (1963).
[12] S. N. Majumdar, D. S. Dean, and P. Grassberger, Phys. Rev. Lett. **86**, 2301 (2001).
[13] N. Menyhárd and G. Ódor, Phys. Rev. E **66**, 016127 (2002).
[14] N. Menyhárd and G. Ódor, Phys. Rev. E **68**, 056106 (2003).
[15] R. B. Griffiths, Phys. Rev. Lett. **23**, 17 (1969).
[16] R. Cafiero, A. Gabrielli, and M. A. Muñoz, Phys. Rev. E **57**, 5060 (1998).
[17] R. Dickman and A. Y. Tretyakov, Phys. Rev. E **52**, 3218 (1995).
[18] M. A. Burschka, C. R. Doering, and D. ben-Avraham, Phys. Rev. Lett. **63**, 700 (1989).
[19] V. Elgart and A. Kamenev, Phys. Rev. E **74**, 041101 (2006).
[20] R. L. Jack, P. Mayer, and P. Sollich, J. Stat. Mech.: Theory Exp. 2006, P03006.
[21] O. Al Hammal, J. A. Bonachela, and M. A. Muñoz, J. Stat. Mech.: Theory Exp. 2006, P12007.
[22] I. Webman, D. ben-Avraham, A. Cohen, and S. Havlin, Philos. Mag. B **77**, 1401 (1998).
[23] A. J. Noest, Phys. Rev. Lett. **57**, 90 (1986); Phys. Rev. B **38**, 2715 (1988).
[24] J. Hooyberghs, F. Iglói, and C. Vanderzande, Phys. Rev. Lett. **90**, 100601 (2003).
[25] G. Ódor and N. Menyhárd, Phys. Rev. E **61**, 6404 (2000).
[26] B. P. Lee, J. Phys. A **27**, 2633 (1994).
[27] G. M. Schütz and K. Mussawisade, Phys. Rev. E **57**, 2563 (1998).
[28] P. Le Doussal and C. Monthus, Phys. Rev. E **60**, 1212 (1999).
[29] G. Ódor and N. Menyhárd, Physica D **168**, 305 (2002).
[30] B. P. Lee and J. Cardy, J. Stat. Phys. **80**, 971 (1995).